Supercapacitors aging assessment in wind/tidal intermittent energies application with variable temperature

Cheikh Tidiane Sarr, Mamadou Baïlo Camara, Brayima Dakyo

Supercapacitors aging assessment in wind/tidal intermittent energies application with variable temperature

Cheikh Tidiane SARR*; Mamadou Baïlo CAMARA*; and Brayima DAKYO
GREAH Laboratory, University of Le Havre Normandy
75 Rue Bellot, 76600 Le Havre, FRANCE

Abstract —**This paper presents the supercapacitors characterization and modeling considering the influence of the intermittent current's ripple rate, the temperature and cycling factor. The aim of the study is to propose supercapacitors aging model that can be used in adaptive energy management based on the micro-grid power fluctuations mitigation in variable temperature conditions. The model of the supercapacitors is dedicated to multi-source systems such as distributed power generation systems based renewable energies (wind, tidal and/or photovoltaic). Energetic performances of the supercapacitors used in these systems can be altered by the critic temperatures and intermittency of the supercapacitors current allocated to the micro-grid power fluctuations mitigation due to renewable energies. Paper contribution is focused on the supercapacitors parameters degradation study according to the combination of the intermittent current's ripple rate, the temperature and the number of the cycles. Experimental tests are performed through charge/discharge operations using intermittent current waveforms with several temperature conditions. Experimental data are like to simulations outcomes with a good concordance. Therefore, the proposed model is adequate to describe the degradation of the supercapacitor's parameters due to intermittent current and using temperature.**

***Keywords*: Micro-grid power fluctuations mitigation, Supercapacitor energy storage, Supercapacitor aging characterization, Supercapacitor aging modeling, Intermittent current, Variable temperature**

Appendix A. Abbreviations

SC	Supercapacitor
V_{sc}	Supercapacitors module voltage in (V)
I_{sc}	Current of the supercapacitor in (A)
N_{cy}	Number of charge/discharge cycles
τ	Current ripple rate
T	Supercapacitors operating temperature in (°C)
ESR (τ, T, N_{cy})	Resistance of the supercapacitor cell in (Ω)
C (τ, T, N_{cy})	Capacitance of the supercapacitor cell in (F)
Δ_{ESR}	Relative error of ESR (τ, T, N_{cy}) in (%)
Δ_C	Relative error of C (τ, T, N_{cy}) in (%)
I_{ave}	Average value of the intermittent current in (A)
I_{max}	Maximum value of the intermittent current in (A)
I_{min}	Minimum value of the intermittent current in (A)
ΔI	Intermittent current variation ranges in (A)
HF	High frequency component of the currents
LF	Low frequency component of the currents

Corresponding author*: E-mail addresses: dikelsarr00@gmail.com (C.T.Sarr*), camaram@univ-lehavre.fr (M.B.Camara*), brayima.dakyo@univ-lehavre.fr (B. Dakyo) .

1. Introduction

Supercapacitors are considered as a power source, with a power density between 5 and 15kW/kg. Today, they cannot compete with the batteries in terms of energy density. Indeed, the electric energy is directly stored in electrostatic form without particular energy conversion. Therefore, the stored electric energy can be rapidly supplied by supercapacitors. Although their specific energy amount is rather low (about 5-10Wh/kg), SCs present the high-power density and outstanding cycling capability. They are able to provide high levels of current and power for about one million charge/discharge cycles in normal using conditions. Their applications are large such as wireless sensor networks, space vehicles, decentralized energy production based on renewable energies [1], [2], [3], hybrid and electric vehicles [4], and uninterrupted power supplies. They are also complementary to the batteries or the fuel cells with different dynamic behavior and energy storage capability [5], [6], [7], [8] and [9].

To maximize the renewable energies integration in the electric grids without a degradation of energy quality is a key challenge. Problem is due to the growth of distributed energy sources integrating intermittent renewable energy sources such as tidal energy, wind energy and photovoltaic systems. To obtain a good correlation between the distributed energy production and quality requirement of the customers using Supercapacitors Energy Storage System (SESS) is an adapted solution. Using SESS to mitigate the intermittent energy due to the renewable energy sources can accelerate the SESS aging, especially in the critic temperature using conditions. This issue is addressed in this paper to propose an adapted electric model of the SESS dedicated to adaptive energy management. SESS model will be based on the characterization data obtained in combined conditions of the current ripple rate and the variable temperature. In the literature, several authors have done the supercapacitors characterization and modeling for different purposes. In Ref. [10], the authors do the SC characterization to show the electrochemical changes in the supercapacitors over time, that is to say by analyzing the impedance variation, in order to suggest aging models. In Ref.[11], authors track the evolution of the parameters in relation to the life-time and temperature combination. In Ref. [12-13], the authors consider the parameters evolution based on calendar tests in order to predict the degradation of the supercapacitors. The authors of [14] use impedance spectroscopy method to develop a thermal model of the SC parameters as a function of frequency for different temperatures. In Ref. [15],[16],[17], the authors present the impact of the temperature on the supercapacitors parameters. Aging characterization of the supercapacitors in

time domain is performed in [16] using electro-thermal stresses defined by the combination of the temperature and the frequency of the DC current ripples. In Ref. [18], the authors do the SC characterization in order to determine the parameters evolution according to the aging and the temperature. In Ref. [17], [19], authors estimate the online lifetime of supercapacitors. The online technique uses a Lyapunov based adaptation law to determine online the capacitance of the SC. Estimated capacitance is expressed as a function of voltage and temperature. In Ref. [20], the authors propose a SC prediction aging model based on voltage and temperature for telecommunications applications. The authors report on the variation of capacitance and ESR based on these constraints to express the aging process. The authors used the cycling principle to determine the life cycle of the supercapacitors. They go up to 25000 cycles to account for the evolution of parameters. Others models of the supercapacitors based on the tram regenerative braking system, the non-idealities of the energy storage system, the dynamic equivalent circuit with a distribution of relaxation times, and the SC self-discharging are presented in [21-24]. The contributions of the paper compared to the works in the literature are focused on two aspects: -First is the supercapacitor's parameters degradation study according to the combination of the intermittent current's ripple rate, the temperature and the number of the cycles. -The second is the electric aging behavior modeling based on the current ripple rate, the temperature and the number of the cycles.

Paper is organized as follows: in section 2, experimental tests bench and the SC characterization method are presented. Tests protocol and supercapacitors parameters aging assessment are introduced in section 3, where the test conditions and results are presented. In section 4, the performances of the proposed SC model are presented with discussions. Finally, conclusions are done in section 5.

2. Experimental setup and characterization method

2.1. Experimental setup

Fig.1 shows the used tests bench for SC characterization. This equipment includes: a SC cycler based BT2000 system used for cycling tests with intermittent current; an impedance spectroscopy based Modulab-XM-system; an ARS-0220 climatic chamber for temperature control and external power booster 50V/25A to boost the current of the spectrometer. Indeed, the current in the spectrometer without booster is a few milli-amperes. It is necessary to boost the current in order to have a significant current corresponding to real electric applications. SC characterization is performed through Electrochemical Impedance Spectroscopy (EIS). In our case, the swept frequencies range is 10 mHz ~ 1kHz. This range of the frequencies is used to determine the supercapacitors resistance and capacitance.

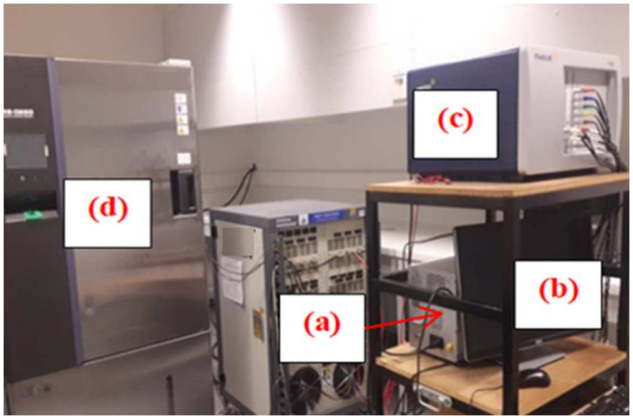

Fig.1. Experimental setup: (a) external booster, (b) computer, (c) Modulab-XM-System and (d) climatic chamber.

2.2. Normalized resistance and capacitance of the supercapacitors according to the number of cycles

Fig.2 and Fig.3 present respectively the evolution of the normalized resistance and normalized capacitance as a function of the number of cycles. The tests are done for 14000 cycles. Resistance *ESR* and capacitance *C* are estimated for each 2000 cycles. The tests are done with constant current of ±20A in charge/discharge operations. Tests protocol and the resistance/capacitance identification method are described in Ref. [19].

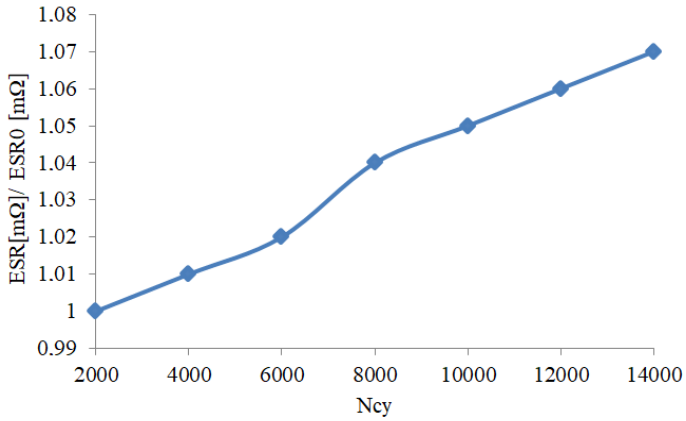

Fig.2: Evolution of normalized resistance as function of the number of cycles.

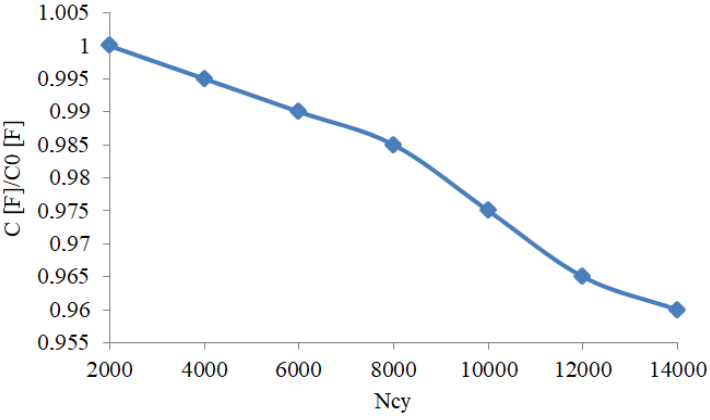

Fig.3: Evolution of the normalized capacitance as function of the number of cycles.

$$\begin{cases} K_{Ncy} = \dfrac{ESR}{ESR_0} = \alpha.\exp(\lambda.N_{cy}) \\ Q_{N_{cy}} = \dfrac{C}{C_0} = \beta.\exp(-\mu.N_{cy}) \\ \alpha = 0.9879 \;;\; \lambda = 6*10^{-06}\;; \\ \beta = 1.01\;;\; \mu = 5*10^{-06} \end{cases} \quad (1)$$

The model of the normalized resistance and the capacitance obtained from experimental data is presented in equation (1), where N_{cy} is the number of charge/discharge cycles, where α, β, μ and λ are the fitting coefficients.

2.1. *Supercapacitors current profile and current ripple rate formulation*

SC cell cycling tests are based on a fluctuating current profile with an average current of I_{ave} as illustrated in Fig.4, where the waveform is limited by I_{max} and I_{min}. DC current ripple rate (τ) is computed using equation (2). The dependency of the SC resistance/capacitance as a function of the current ripple rate is described in a previous paper [19].

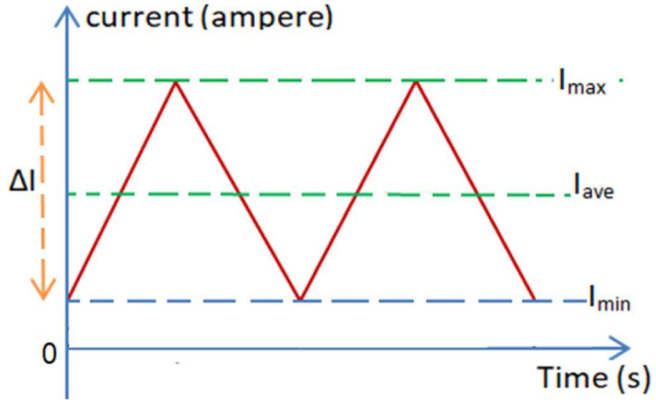

Fig.4: Fluctuating DC-current waveform.

$$\tau = \frac{\Delta I}{2 . I_{ave}} = \frac{(I_{max} - I_{min})}{2 . I_{ave}} \quad (2)$$

2.2. *Supercapacitors parameters identification method*

SC characterization is performed with an impedance spectroscopy which allows precise knowledge of the time constants of the equivalent circuit. Impedance spectroscopy is a powerful technique for characterizing batteries or supercapacitors. It is based on the application of a sinusoidal variable signal of low magnitude to obtain a sinusoidal output response as illustrated in Fig.5. Current and voltage are the two physical signals used to characterize an electrochemical cell. Thus, the excitation signal can be the voltage or the current, that makes it possible to obtain two particular modes of characterization. The potentiostatic mode is based on the application of a sinusoidal voltage excitation and to follow the current response. Conversely, the galvanostatic mode uses a current excitation and leads to measure the voltage response. The potentiostatic mode is used in this paper because in the case of SC, the operating point is directly related to the DC-voltage of the supercapacitors. The resistance and capacitance of the supercapacitors are obtained from the impedance measurement based on flowchart presented in Fig.5 and using equation (3), where $I_m(z)$ is the imaginary component and $R_e(z)$ is the real component of the SC impedance. The capacitance is calculated at low frequency (here10 mHz) according to [10]. Supercapacitors aging tests are performed using a Boostcap 3000F/2.7V supercapacitor cell at 25°C with a variable magnitude-triangular current profile with a frequency of 500 mHz as presented in Fig.6. After each 500 cycles of charge/discharge, the resistance *ESR* and

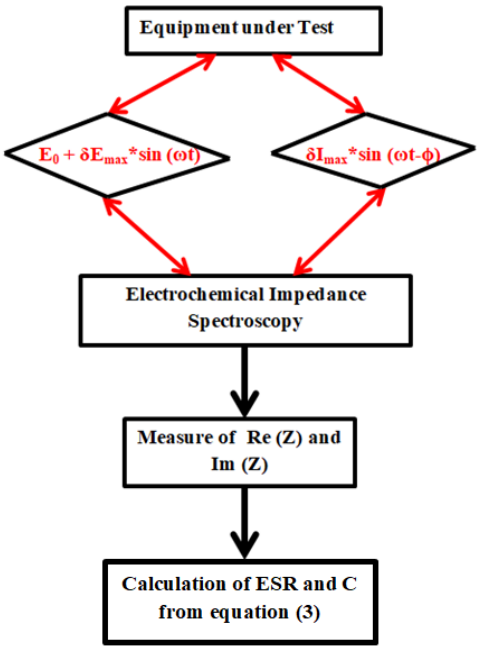

Fig.5: Impedance spectrometry method.

$$\begin{cases} C = -\dfrac{1}{2 . \pi . I_m(z) . f} \\ ESR = \min(R_e(z)) \end{cases} \quad (3)$$

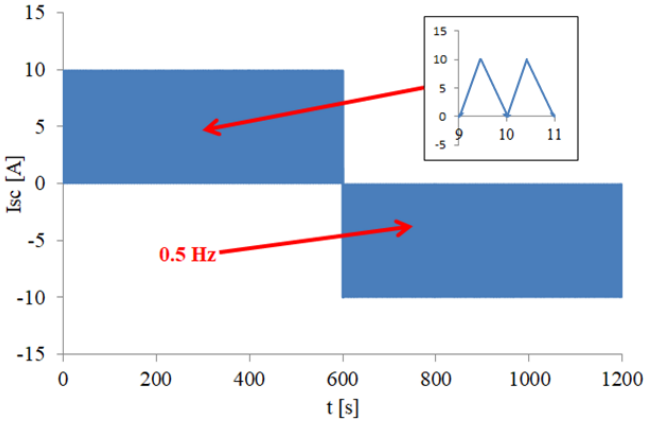

Fig.6: Example of the used current profile for SC cycling tests.

capacitance *C* of the SC are computed from the impedance measurement based on potentiostatic mode, using equation (3).

3. Tests protocol and supercapacitor's parameters aging assessment

3.1. *Tests protocol*

For this study, the SC cell is confined in a controlled climatic chamber with a temperature range of -60°C to +180°C. This climatic chamber allows varying the temperature during the tests. For each test, the SC cell is putted in the climatic chamber for the time necessary for inside temperature stabilization before starting the electric cycling tests. Fig.7 illustrates the experimental tests protocol flowchart based on the variable temperatures. Tests are performed using a triangular current profile with frequency of 0.5 Hz and current

ripple rate of 100% compared to an average value of 20A. After each 250 of charge/discharge cycles the impedance of the SC is measured to compute the resistance ESR and capacitance C as illustrated in Fig.7. The same process is repeated for following temperatures: -40°C, -30°C, -20°C, -5°C, 10°C, 20°C, 30°C, 45°C, 55°C and 65°C.

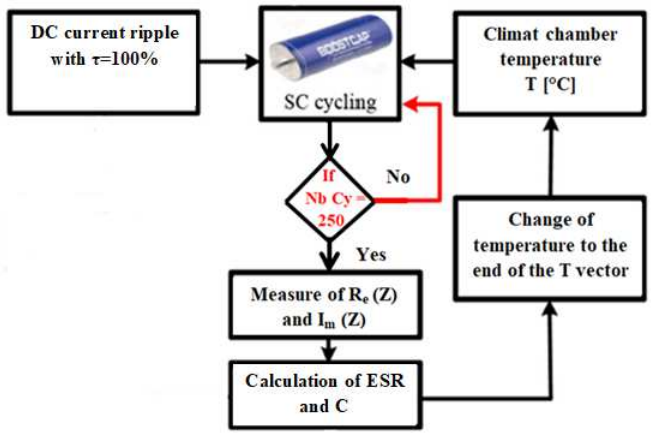

Fig.7: SC characterization process using constant current ripple rate with variable temperatures.

3.2. Resistance and capacitance aging assessment according to the using temperature

Fig.8 and Fig.9 illustrate the variations of the resistance and capacitance of the aged SC as function of the using temperature. These figures show that *ESR* decreases when the temperature is between -40°C and 0°C, and exponentially grows for the positive temperatures between 0°C and 65°C. The reverse phenomenon is noticed for SC capacitance plotted in Fig.9, where the capacitance increases between -40°C and -5°C, and it decreases between -5°C and 65°C. At the end of the tests with the temperatures, the series resistance *ESR* has increased about 0.138 mΩ corresponding to an increasing of 34% compared to its minimum value (0.28 mΩ). Otherwise, the capacitance has decreased about 403F corresponding to a decrease of 13% compared to its maximum value. These curves are parabolic form with minimal resistance ESR_{min} at 0ºC and maximal capacitance C_{max} at -5ºC. Therefore, the temperature has a significant influence on the supercapacitors aging. At high temperatures, the SC equivalent series resistance increases and its capacitance decreases. The high temperatures tend to cause side reactions to take place at the electrode / electrolyte interface of the SC between the electrolyte ions and the functional groups. The functional groups are generally composed of carboxyl, lactone and phenol groups. The interaction of the latter with the organic electrolyte leads to side reactions with the formation on the surface of the latter of substances capable of blocking the entrance to the pores. This causes the reduction of the pore surface area promoting a loss of active material coinciding with the drop of the capacity. The increase in serial resistance under the effect of high temperatures, for its part, results from the formation of gas molecules, which are mostly methane, ethane, dioxygen and hydrogen, during the reaction functional groups with the electrolyte. Unlike solid substances, these gaseous molecules are likely to be absorbed in the pores or to circulate freely in the cell, thus creating pressure inside the case and causing deterioration of the electrode. They also have the effect of blocking the pores of the separator, which slows down the transfer of ions and therefore increases the macroscopic electrical resistance [25], [26], [27]. Generally, the SC is said to be aged when its resistance has increased in order to 100% compared to its initial value and its capacitance decreases of 20% of its initial value. Fig.8 and Fig.9 show the SC cell presents a different behavior as function of the positive and the negative temperatures.

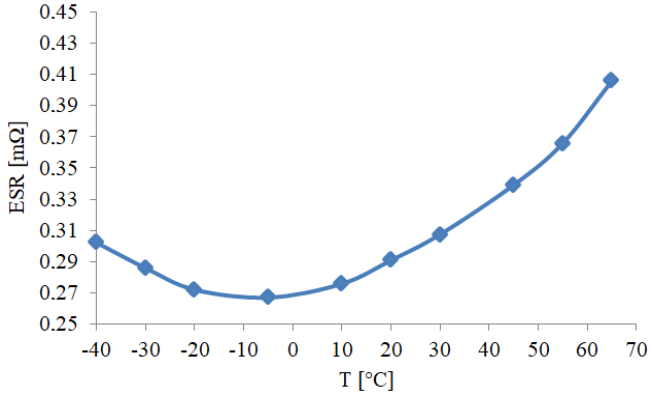

Fig.8: Evolution of the SC series resistance *ESR* according to the temperature.

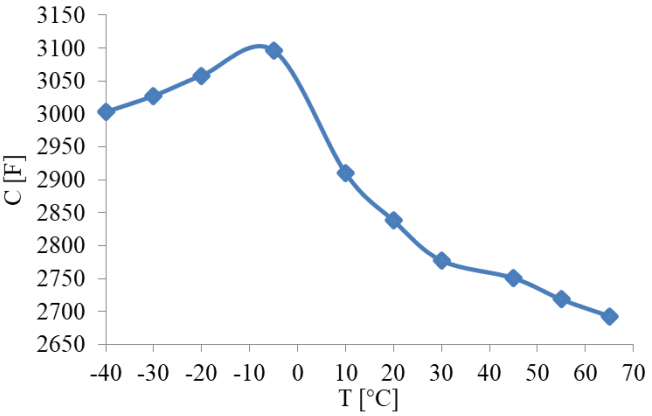

Fig.9: Evolution of the *SC* capacitance *C* according to the temperature.

3.3. Resistance and capacitance of the supercapacitors according to the current magnitude

In this section, the authors propose to use the different currents magnitudes in SC characterization to show the impact of the current scale factor.

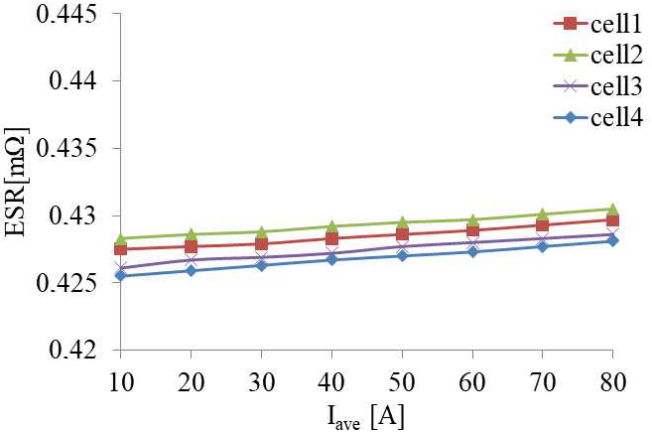

Fig.10: Evolution of the SC resistance according to the current magnitude.

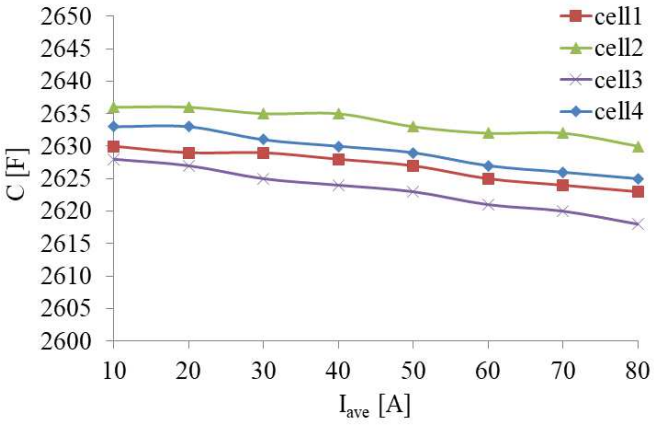

Fig.11: Capacitance of the SC according to the current magnitude.

For all tests with the currents from 10A to 80A, the resistances of the cells are between 0.425mΩ and 0.43mΩ as illustrated in Fig.10. For all cells, the resistance can be considered as quasi-constant because the variations of the *ESR* compared to its initial value do not exceed 1%. For all cells illustrated in Fig.11, the variations of the capacitance are little (from 2635F to 2605F) compared to initial value, i.e. it is not exceeding 1%. So, the capacitance can be also considered as quasi-constant. Based on Fig.10 and Fig.11, this section can be concluded as following: the current magnitude has not significant impact on the SC resistance and its capacitance. Same observation is done in [16].

3.4. Resistance and capacitance of the supercapacitors according to the current ripple rate and the temperature

The tests are done using 4 Boostcap 3000F/2.7V new supercapacitors cells for the positive temperatures and 4 new cells for the negative temperatures. Used temperatures for SC characterization are: -40°C, -30°C, -10°C, -5°C, 10°C, 20°C, 30°C, 45°C, 55°C and 65°C. Used current ripple rate (τ) are: 20%, 40%, 60%, 80% and 100%. Full tests are done for 5000 cycles of charge/discharge with different temperature and different τ, so 500 cycles for each temperature. Experimental results of the average value from the 8 cells, using positive and negative temperatures and τ are presented in Fig.12 to Fig.15.

Fig.12 and Fig.13 illustrate respectively the evolution of the resistance *ESR* and capacitance *C* according to the τ and the negative temperatures. Fig.12 shows a non-linear behavior of the *ESR* as function of the negative temperature and the current ripples rate τ. The resistance decreases about 0.0421mΩ between -40°C at 20% of current's ripples rate and -5°C at 100%, so 14% compared to its initial value. In other terms, the resistance of the SC decreases if the using temperature is negative and τ increases. Based on Fig.13, between – 40°C at 20% and -5°C at 100% of current's ripples rate, the average capacitance of the four cells increases in order of 124F. This variation corresponds an increasing of 4% compared to its initial value. For conclusion, the capacitance of SC cell increases if the using temperature is negative and τ increases.

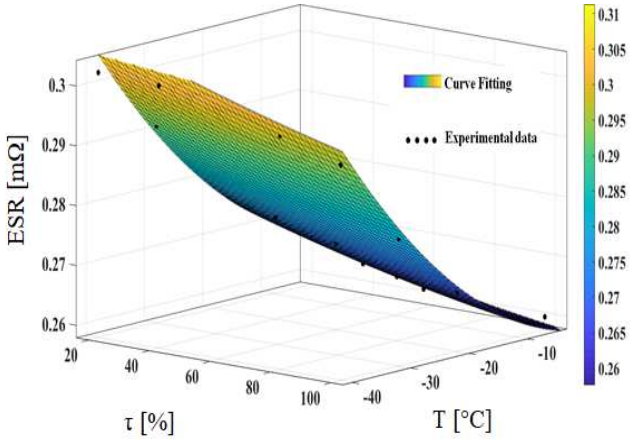

Fig.12: *ESR* from 4 cells as function of negative temperature and τ.

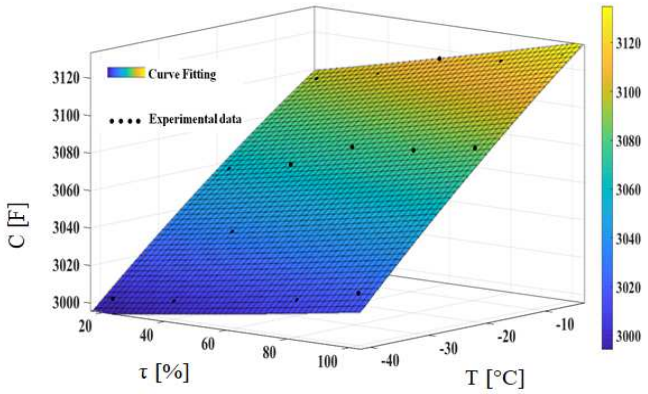

Fig.13: Capacitance from 4 cells as function of negative temperature and τ.

In other terms, the combination of the τ and the negative temperatures affects the SC resistance and the capacitance of the SC. When the SC cell is maintained at negative temperatures, it tends to regenerate its capacitance and decreasing the *ESR*.

The SC resistance and the capacitance evolutions according to the positive temperatures and τ are respectively presented in Fig.14 and Fig.15. These figures show a good correlation between the interpolated curves and the experimental data. Fig.14 shows a non-linear behavior of the SC resistance when the using temperature is positive with a variable current ripples rate.

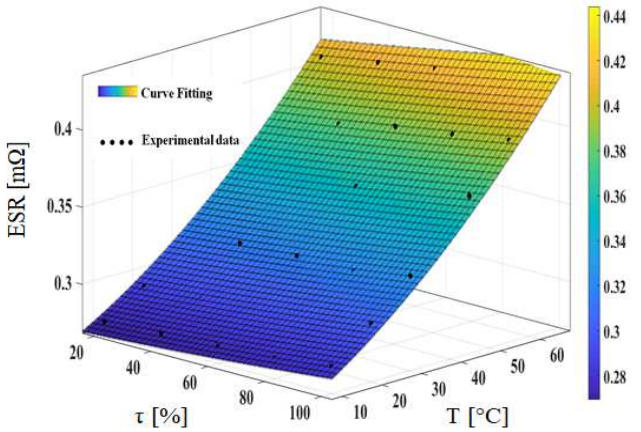

Fig.14: Resistance from 4 cells according to positive temperature and τ.

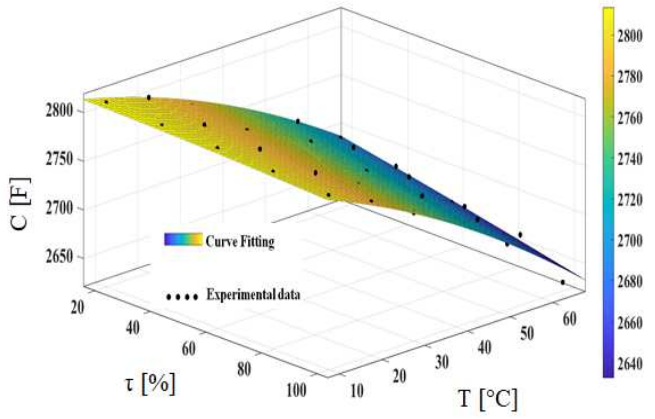

Fig.15: Capacitance from 4 cells according to positive temperature and τ.

Average resistance of SC cells increases in order of 0.152mΩ between 10°C at 40% and 65°C at 100%, so an increasing of 64.5% compared to initial conditions. Fig.15 shows that, the average capacitance of the SC cells decreases in the order of 180F between 10°C at 20% and 65°C at 100%, which correspond to a decreasing of 9% compared to its initial value.

Fig.14 and Fig.15 show that, a combination of the variable current's ripples rate and the positive temperatures degrades the resistance and capacitance of the SC. Compared to the current's ripples rate, the temperature has more impact on degradation of the SC resistance and its capacitance [19]. The models of the average resistance and the average capacitance obtained from the experimental data based on 250 cycles are presented in the equations (4) and (5), where T is the using temperature which can be positive or negative and τ is the current's ripples rate of the fluctuating DC-current.

$$ESR(\tau,T)=\begin{cases}(k_0+k_1.\tau+k_2.T+k_3.\tau^2+k_4.\tau.T+k_5.T^2) & T\geq 0\\ (k_6+k_7.\tau+k_8.T+k_9.\tau^2+k_{10}.\tau.T+k_{11}.T^2) & T<0\end{cases} \quad (4)$$

$$C(\tau,T)=\begin{cases}(a_0+a_1.\tau+a_2.T+a_3.\tau^2+a_4.\tau.T+a_5.T^2) & T\geq 0\\ (a_6+a_7.\tau+a_8.T+a_9.\tau^2+a_{10}.\tau.T+a_{11}.T^2) & T<0\end{cases} \quad (5)$$

The fitting coefficients of $ESR(\tau, T)$ and $C(\tau, T)$ are given as following:

- k_0=-0.06; k_1=0.03; k_2=-6.47*10^{-04}; k_3=-5.51*10^{-04}; k_4=9.26*10^{-05}; k_5=1.56*10^{-05}; k_6=0.68; k_7=-0.03; k_8=-4.27*10^{-04}; k_9=7.67*10^{-04}; k_{10}=1.18*10^{-05}; k_{11}=1.95*10^{-05};
- a_0=3111; a_1=26.33; a_2=4.46; a_3=0.59; a_4=-0.26; a_5=-0.01; a_6=3063; a_7=8.90; a_8=39.08; a_9=-1.96; a_{10}=1.74; a_{11}=1.86.

An extrapolation of equations (4) and (5) for 14000 cycles of the SC charge/discharge is presented in equations (6) and (7), where K_{Ncy} and Q_{Ncy} present the aging factor obtained from the experimental data plotted respectively in Fig.2 and Fig.3.

$$ESR(\tau,T,N_{cy}) = K_{N_{cy}} * ESR(\tau,T) \quad (6)$$

$$C(\tau,T,N_{cy}) = Q_{N_{cy}} * C(\tau,T) \quad (7)$$

3.5. Electric behavior model of the supercapacitors based on aging assessment

Verifications of the SC model are performed using the temperature, the current's ripples rate and the number of the charge/discharge cycles. Obviously, the number of the SC charge/discharge cycles is an intrinsic constraint because we cannot do the tests without cycling. It has been observed during the experimental tests, the resistance *ESR* and the capacitance *C* of the SC vary according to the number of cycles. Fig.16 presents the proposed model of the SC cell which includes a series resistance $ESR(\tau,T,N_{cy})$, and a variable capacitance which includes $C(\tau,T,N_{cy})$ and $\chi_v.V$.

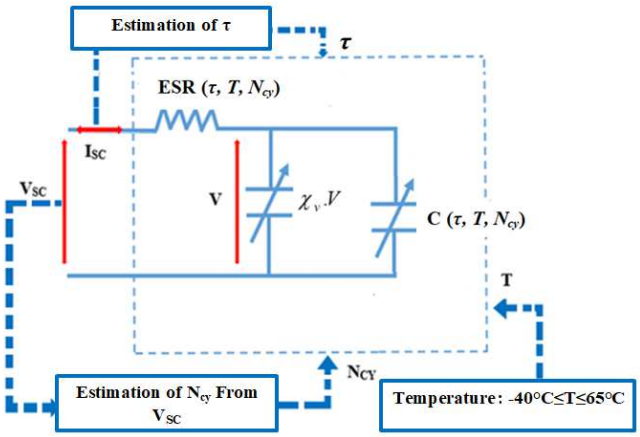

Fig.16: Behavior model of the supercapacitor cell.

Mathematical model of the SC module is shown in equation (8), where V_0 presents the initial voltage, N_S and N_P present respectively the number of the SC cells in series and in parallel, χ_v is a specific coefficient, and R_{wi} is the resistance due to electric wiring for one cell. The SC module parameters are presented in Table.1.

$$\begin{cases} C_{eq}(\tau,T,N_{cy}) = \frac{N_p}{N_s}\cdot C_{cell}(\tau,T,N_{cy}) \\ R_{eq}(\tau,T,N_{cy}) = \frac{N_s}{N_p}\cdot ESR(\tau,T,N_{cy}) + \frac{(N_S-1)}{N_p}\cdot R_{wi} \\ C_{cell}(\tau,T,N_{CY}) = C(\tau,T,N_{CY}) + \chi_v.V \\ V_{sc} = N_s\cdot V_0 - \int_0^t \frac{I_{sc}}{C_{eq}(\tau,T,N_{cy})}\cdot dt - R_{eq}(\tau,T,N_{cy})\cdot I_{sc} \end{cases} \quad (8)$$

Table 1. Supercapacitors pack parameters based on Boostcap 3000F/2.7V cell.

Description	Symbol	Parameters
Maximum voltage of the Sc module	V_{Scmax}	*70 V*
Specific coefficient	χ_v	0.077 *V/F*
Number of cells in series	N_s	*26*
Number of cells in parallel	N_P	*1*
Resistance due to electric wiring for one cell	R_{wi}	*2.9 m* Ω

4. Model verifications and discussions

4.1. Efficiency of the supercapacitors model

To evaluate the efficiency of the model compared to the experimental data, the authors propose a comparative study between the simulations and experimental results as summarized in Table.2 and Table.3. Considering other operating points (temperature, current ripples rate, and number of cycles) in the simulations enables to show the efficiency of the proposed model compared to experimental tests results. Table.2 and Table.3 show, for a temperature of -35°C with a current's ripples rate of 20% at 250 cycles, the SC cell parameters from the simulations and the experiment test are

close with a relative error compared to experimental data of 0.019% for the resistance, and 0.026% for the capacitance. Table.2 and Table.3 show that at 13000 cycles, the results from experimental tests and simulations ones are close with a relative error compared to experimental data of 0.009% for the resistance and 0.032% for the capacitance.

Table.2: Resistance of the SC from experimental and simulations tests.

Test conditions			Resistance		
τ [%]	T[° C]	Ncy	ESR_{Sim} [mΩ]	ESR_{Exp} [mΩ]	Δ_{ESR} [%]
20	35	250	0.301	0.295	0.019
40	-25	250	0.289	0.287	0.006
60	35	250	0.280	0.312	0.103
80	60	250	0.350	0.370	0.055
100	45	13000	0.539	0.523	0.009

Table.3: Capacitance of the SC from experimental and simulations tests.

Test conditions			Capacitance		
τ [%]	T[°C]	Ncy	C_{Sim} [F]	C_{Exp} [F]	Δ_C [%]
20	35	250	2930	3007	0.026
40	-25	250	2960	3033	0.020
60	35	250	2770	2765	0.002
80	60	250	2670	2703	0.012
100	45	13000	2660	2686	0.032

Based on the outcomes presented in Table.2 and Table.3, the proposed model is adapted to extrapolate for a high number of the cycles and does not require very long experimental tests to estimate the resistance and capacitance variations.

4.2. Dynamics performances assessment

The dynamics performances assessment of the model is evaluated using a current's profile resulting from an energy management strategy based on wind and tidal turbines system. The configuration of the system is illustrated in Fig.17, and the considered energy management is based on the frequency approach.

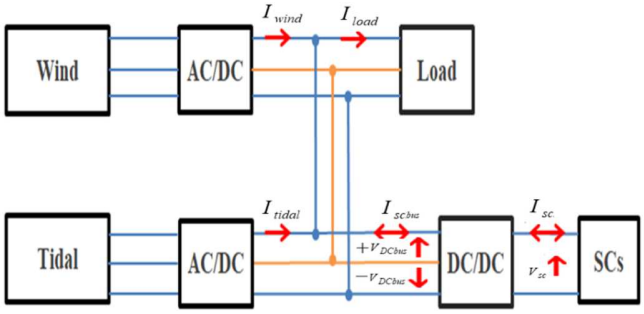

Fig.17: Configuration of the system based on Vienna AC/DC rectifiers, DC/DC converter and supercapacitors.

The principle of the energy management based on the frequency approach consists to allocate the high frequency component of the power from the wind and the tidal to the pack of supercapacitors. In comparison with the different electrical energy management approaches proposed in the literature [28], [29], [30], the particularity of the frequency approach lies in considering the strengths and weaknesses energy sources by sharing the load demand according to the power and energy densities of each of the sources involved. In other words, the objective of the paper is to characterize the aging of supercapacitors under the action of fluctuations in currents. The issue is not energy management but only how can we obtain the high frequency components of the currents from the wind turbine, tidal turbine and the load. In this case, the choice of energy management approach is based on the possibility of extracting high frequency fluctuations from energy supply and demand. Among the energy management methods proposed in the literature, the frequency approach is most suitable for extraction of the high frequency components of the currents. It allows guarantee the high frequency currents components allocation to SC. The concept of the energy management based on the frequency approach is described in [31].

Fig.18, Fig.19 and Fig.20 present respectively the contributions of the wind turbine I_{wind}, the tidal turbine I_{tidal} and the load demand I_{load}. The current of the SC corresponding to the high frequency component dedicated to power fluctuations compensation in DC-bus added to an average component is presented in Fig.21. This current profile can be expressed as shown in equation (9), where the index "*HF*" presents the high frequency component of the currents and "*LF*" is the low frequency component. To ensure a full charge/discharge cycle of the supercapacitors, a variable offset component I_{offset} is added to the high frequency components from the wind energy, tidal energy and the load demand as presented in equation (9). This offset is positive for the SC charge operations and it is negative for the SC discharge operations. The experimental tests are done using current profile presented in Fig.21 at 65°C and -40°C.

$$\begin{cases} I_{wind} = I_{wind_{HF}} + I_{wind_{LF}} \\ I_{tidal} = I_{tidal_{HF}} + I_{tidal_{LF}} \\ I_{load} = I_{load_{HF}} + I_{load_{LF}} \\ I_{load_{LF}} = I_{wind_{LF}} + I_{tidal_{LF}} \\ I_{scref} = \frac{V_{DCbus}}{V_{sc}} \cdot \left(I_{load_{HF}} - \left(I_{wind_{HF}} + I_{tidal_{HF}} \right) \right) + I_{offset} \end{cases} \quad (9)$$

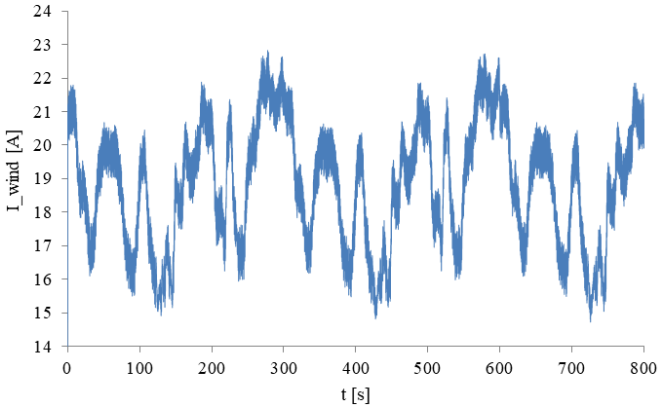

Fig.18: Contribution of the wind turbine in the DC-bus.

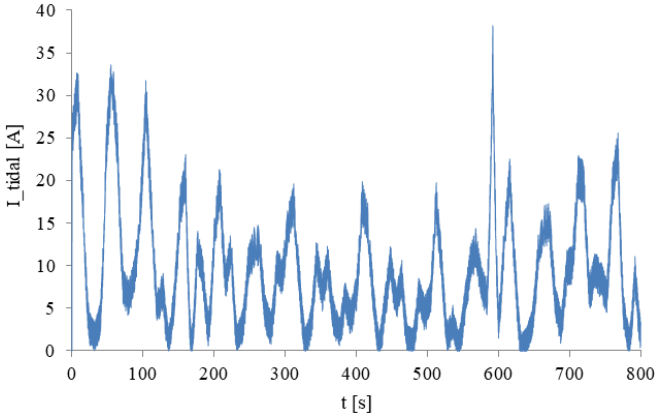

Fig.19: Contribution of the tidal turbine in DC-bus

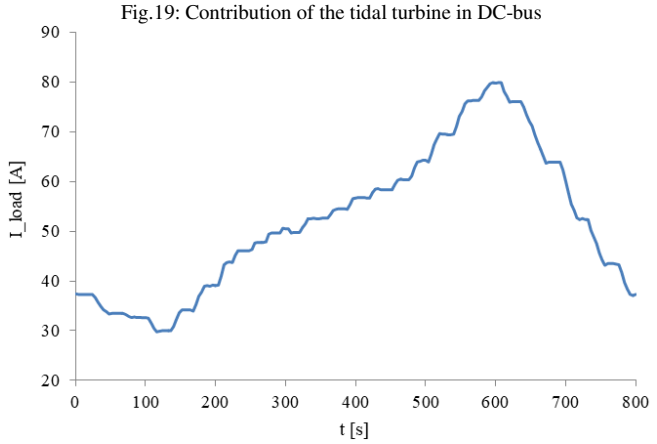

Fig.20: Load demand in DC-bus

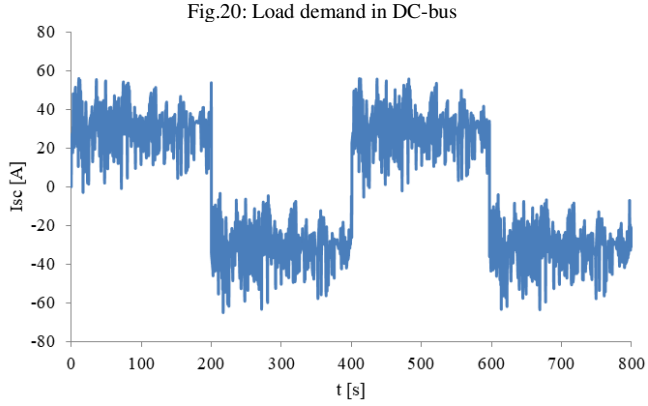

Fig.21: Supercapacitors current profile with I_{offset} of ±30A.

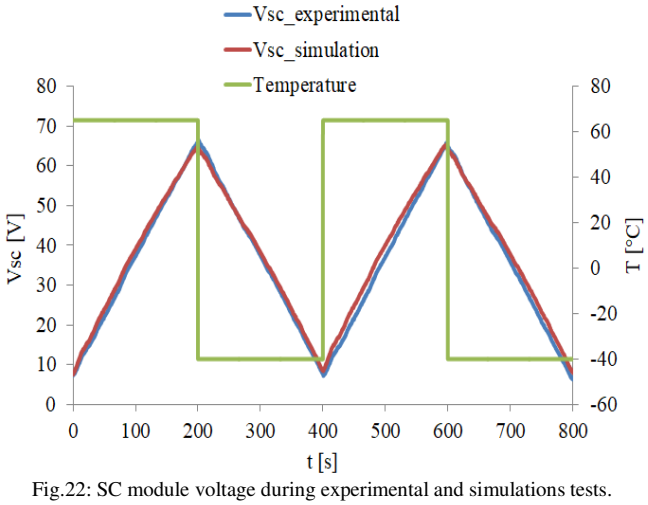

Fig.22: SC module voltage during experimental and simulations tests.

Fig.22 shows the terminal voltage of the SC module obtained from the experimental and simulations tests, where the simulations and experiment outcomes are close. However, the proposed model is adequate to describe the SC behavior during the charge /discharge operations for a temperature range of -40 to 65°C, with a variable current's ripples rate. In fact, as illustrated in the tables 2 and 3, for tests carried out at 250 cycles, the proposed model is able to compute the SC parameters at 13000 cycles or more without doing experimental tests.

5. Conclusions

Used method for the supercapacitors characterization is based on the frequency domain. The obtained results from Electrochemical Impedance Spectroscopy show that the resistance and capacitance depend on the number of cycles, the temperature and the current ripples rate. For the temperature point of view, the SC resistance and its capacitance present parabolic variations. In fact, for negative temperatures, the resistance decreases and the capacitance increases. But for the positive temperatures, the reverse evolution is observed. This parabolic evolution is observed when the temperature is combined with the current ripples rate. The resistance of the SC decreases and its capacitance increases as function of the current's ripples rate increase for the negative temperatures. A reverse behavior is observed for the positive temperatures. The proposed model is suitable to describe the variations of the SC resistance and its capacitance as a function of the temperature and current's ripples rate, for more than 14000 charge/discharge cycles. Based on these results, we can conclude that the temperature, the number of cycles and current's ripples rate are the key parameters which can affect the supercapacitors aging.

Acknowledgment

The authors would like to thank the Council of the Region Normandy/France, University of Le Havre Normandy and the Council of the European Union for their financial support.

References

[1] A.Bouakkaz, A.J. Gil Mena, S.Haddad, M.L. Ferrari, Efficient energy scheduling considering cost reduction and energy saving in hybrid energy system with energy storage, Journal of Energy Storage 33 (2021) 101887, https://doi.org/10.1016/j.est.2020.101887

[2] C.Wang, Z.Zhang , O.Abedinia, S.G. Farkoush, Modeling and analysis of a microgrid considering the uncertainty in renewable energy resources, energy storage systems and demand management in electrical retail market, Journal of Energy Storage 33 (2021) 102111, https://doi.org/10.1016/j.est.2020.102111

[3] M.Mühlbauer, O.Bohlen, M.A. Danzer, Analysis of power flow control strategies in heterogeneous battery energy storage systems, Journal of Energy Storage 30 (2020) 101415, https://doi.org/10.1016/j.est.2020.101415

[4] Q.Xun, S.Lundberg, Y.Liu, "Design and experimental verification of a fuel cell/supercapacitor passive configuration for a light vehicle", Journal of Energy Storage 33 (2021) 102110. https://doi.org/10.1016/j.est.2020.102110

[5] K.Bellache; M.B.Camara; B.Dakyo, Transient Power Control for Diesel-Generator Assistance in Electric Boat Applications Using Supercapacitors and Batteries, IEEE J. Emerg. Sel. Top. in Power Elect., Vol.6, no.1, 2018. DOI: 10.1109/JESTPE.2017.2737828.

[6] F.Zhu ; Z.Yang ; H.Xia ; F.Lin, Hierarchical Control and Full-Range Dynamic Performance Optimization of the Supercapacitors Energy Storage System in Urban Railway , IEEE Trans. on Industrial Electronics, Vol.65, no.8, 2018. DOI: 10.1109/TIE.2017.2772174

[7] R.German, A.Sari, O.Briat, J-M. Vinassa , P. Venet, Impact of Voltage Resets on Supercapacitors Aging, IEEE Trans. on Industrial Electronics, Vol.63, no.12, 2016 . DOI: 10.1109/TIE.2016.2594786

[8] V.Lystianingrum, B.Hredzak, et al., On Estimating Instantaneous Temperature of a Supercapacitor String Using an Observer Based on Experimentally Validated Lumped Thermal Model, IEEE Trans. on Energy Conversion, Vol. 30, No. 4, Dec. 2015, Pages 1438-1448. DOI: 10.1109/TEC.2015.2433312

[9] P.Saha; S.Dey; M.Khanra, Modeling and State-of-Charge Estimation of Supercapacitors Considering Leakage Effect, IEEE Trans. on Industrial Electronics, Vol.67, no.1, 2020. DOI: 10.1109/TIE.2019.2897506

[10] H.Ahmad, W.Y.Wan, and D.Isa, Modeling the Ageing Effect of Cycling Using a Supercapacitor-Module Under High Temperature with Electrochemical Impedance Spectroscopy Test, IEEE Trans. On Reliability, vol.68, no.1, 2019. DOI: 10.1109/TR.2018.2869212

[11] D.B. Murray, and J.G. Hayes, Cycle Testing of Supercapacitors for Long-Life Robust Applications, IEEE Trans. on Power Elec., vol.30, no.5, page 2505-2516, May 2015. DOI: 10.1109/TPEL.2014.2373368

[12] M.Marracci, B.Tellini, M.Catelani, L.Ciani Ultracapacitor Degradation State Diagnosis via Electrochemical Impedance Spectroscopy, IEEE Trans. On Instrument. and Measurement, vol.64, no.7, Pages: 1916 – 1921, July 2015. DOI: 10.1109/TIM.2014.2367772

[13] A.E. Mejdoubi, A.oukaour, H.Chaoui, H.Gualous, J.Sabor, Y. Slamani "Prediction Aging Model for Supercapacitor's Calendar Life in Vehicular Applications", IEEE Trans. On Vehicular Technology, Page s: 4253 – 4263, 2015. DOI: 10.1109/TVT.2016.2539681

[14] A.E.Mejdoubi ; H.Chaoui ; J.Sabor ; H.Gualous, Remaining Useful Life Prognosis of supercapacitors Under Temperature and Voltage Aging Conditions, IEEE Trans. on Indus. Electronics, Vol.65, no.5, 2018 . 10.1109/TIE.2017.2767550

[15] Y.Li, S.Wang, Meina Zheng, and Jun Liu, Thermal Behavior Analysis of Stacked-type Supercapacitors with Different Cell Structures, CSEE Journal of Power and Energy Systems, vol.4, No1, Pages: 112 - 120, March 2018. DOI: 10.17775/CSEEJPES.2016.01410

[16] K.Bellache; M.B.Camara, B. Dakyo, Supercapacitors Characterization and modeling using combined electro-thermal stress approach, IEEE Trans. on Industry Applications, vol.65, no.2, 2019. DOI: 10.1109/TIA.2018.2879304

[17] H.Chaoui and H.Gualous, Online Lifetime Estimation of Supercapacitors, IEEE Trans. on Power Electronics, Vol.32, No.9, 2017. DOI: 10.1109/TPEL.2016.2629440

[18] Y.Liu, Z.Huang, H.Liao, C. Lyu, Y.Zhou, Y.Jiao, H.Li, C.Hu, J. Peng, A Temperature-Suppression Charging Strategy for Supercapacitor Stack with Lifetime Maximization, IEEE Trans. on Industry Applications, Vol.55, no.6, 2019. DOI: 10.1109/TIA.2019.2930221

[19] C.T.Sarr, M.B.Camara, B.Dakyo, Influence of cycles number and RMS Value of DC-current Ripple on Supercapacitors Aging, 7th International Conference on Clean electrical Power, 2019 , Otranto, Italy, DOI: 10.1109/ICCEP.2019.8890190

[20] P.Kreczanik, P.Venet, A.Hijazi, and G.Clerc, Study of Supercapacitor Aging and Lifetime Estimation According to Voltage, Temperature, and RMS Current, IEEE Trans. on Indus. Electronics, Vol. 61, no. 9, Sept. 2014. DOI: 10.1109/TIE.2013.2293695

[21] I.Zupan, V.Sunde, Z.Ban, D.Kruˇselj ,Algorithm with temperature-dependent maximum charging current of a supercapacitor module in a tram regenerative braking system, Journal of Energy Storage 36 (2021) 102378, https://doi.org/10.1016/j.est.2021.102378

[22] P. Naresh, N.Sai Vinay Kishore, V. Seshadri Sravan Kumar, Mathematical modeling and stability analysis of an ultracapacitor based energy storage system considering non-idealities, Journal of Energy Storage 33 (2021) 102112, https://doi.org/10.1016/j.est.2020.102112

[23] L.E. Helseth, Modelling supercapacitors using a dynamic equivalent circuit with a distribution of relaxation times, Journal of Energy Storage 25 (2019) 100912, https://doi.org/10.1016/j.est.2019.100912

[24] L.E. Helseth, The self-discharging of supercapacitors interpreted in terms of a distribution of rate constants, Journal of Energy Storage 34 (2021) 102199, https://doi.org/10.1016/j.est.2020.102199.

[25] A. Hammar, P. Venet, R. Lallemand, G. Coquery, and G. Rojat, ''Study of Accelerated Aging of Supercapacitors for Transport Applications'', IEEE Transactions on Industrial Electronics, vol. 57, no. 12, pages. 3972-3979, December 2010. DOI: 10.1109/TIE.2010.2048832

[26] Nagham El Ghossein, Ali Sari, Pascal Venet, ''Effects of the Hybrid Composition of Commercial Lithium-ion Capacitors on their Floating Aging'', IEEE Transactions on Power Electronics, 2018. DOI**:** 10.1109/TPEL.2018.2838678

[27] Hadiza Ahmad, Wong Yee Wan, and Dino Isa, " Modeling the Ageing Effect of Cycling Using a Supercapacitor-Module Under High Temperature With Electrochemical Impedance Spectroscopy Test" IEEE Transactions On Reliability, Pages: 1 - 13 ,2019. DOI:10.1109/TR.2018.2869212

[28] M.Rastegar, M.Fotuhi-Firuzabad, H.Zareipour, M.Moeini-Aghtaieh, ''A Probabilistic Energy Management Scheme for Renewable-Based Residential Energy Hubs'' IEEE Transactions on Smart Grid, Vol.8, no.5, 2017. DOI: 10.1109/TSG.2016.2518920

[29] Md Shahin Alam, Seyed Ali Arefifar, ''Energy Management in Power Distribution Systems: Review, Classification, Limitations and Challenges'', IEEE Access, Vol.7, 2019 DOI: 10.1109/ACCESS.2019.2927303

[30] V.I.Herrera, A.Milo, H.Gaztañaga, A.González-Garrido, H.Camblong, A.Sierra, ''Design and Experimental Comparison of Energy Management Strategies for Hybrid Electric Buses Based on Test-Bench Simulation'', IEEE Transactions on Industry Applications, Vol: 55, no.3, 2019. DOI: 10.1109/TIA.2018.2886774

[31] A. Tani, M. B. Camara, B. Dakyo, Energy Management in the Decentralized Generation Systems Based on Renewable Energy—Ultracapacitors and Battery to Compensate the Wind/Load Power Fluctuations, in IEEE Transactions on Industry Applications, 2014, vol. 51, no 2, p. 1817-1827. DOI: 10.1109/TIA.2014.2354737